LUND UNIVERSITY

Signature of femtosecond laser-induced superfluorescence from atomic hydrogen

Ding, Pengji; Ruchkina, Maria; Wang, Zexuan; Zhuzou, Mingyang; Xue, Shan; Bood, Joakim

Published in:
Physical Review A

DOI:
10.1103/PhysRevA.105.013702

2022

Document Version:
Publisher's PDF, also known as Version of record

Link to publication

Citation for published version (APA):
Ding, P., Ruchkina, M., Wang, Z., Zhuzou, M., Xue, S., & Bood, J. (2022). Signature of femtosecond laser-induced superfluorescence from atomic hydrogen. *Physical Review A*, *105*(1), Article 013702. https://doi.org/10.1103/PhysRevA.105.013702

Total number of authors:
6

General rights
Unless other specific re-use rights are stated the following general rights apply:
Copyright and moral rights for the publications made accessible in the public portal are retained by the authors and/or other copyright owners and it is a condition of accessing publications that users recognise and abide by the legal requirements associated with these rights.
• Users may download and print one copy of any publication from the public portal for the purpose of private study or research.
• You may not further distribute the material or use it for any profit-making activity or commercial gain
• You may freely distribute the URL identifying the publication in the public portal

Read more about Creative commons licenses: https://creativecommons.org/licenses/

Take down policy
If you believe that this document breaches copyright please contact us providing details, and we will remove access to the work immediately and investigate your claim.

LUND UNIVERSITY

PO Box 117
221 00 Lund
+46 46-222 00 00

Download date: 12. Oct. 2024

Signature of femtosecond laser-induced superfluorescence from atomic hydrogen

Pengji Ding,[1,2,*] Maria Ruchkina,[2] Zexuan Wang,[1] Mingyang Zhuzou,[1] Shan Xue,[1,†] and Joakim Bood[2]
[1]*School of Nuclear Science and Technology, Lanzhou University, 730000 Lanzhou, China*
[2]*Division of Combustion Physics, Department of Physics, Lund University, Box 118, SE-221 00 Lund, Sweden*

(Received 29 September 2021; accepted 13 December 2021; published 3 January 2022; corrected 22 February 2022)

Cavity-free lasing generation from gas constituents has been studied in the past decade since it promises great potentials in remote sensing and optical diagnostics techniques. Here we report on experimental investigations of temporal characteristics of H-atom lasing emission at 656 nm by examining the dependences of its durations and delays on the pump-laser-pulse energies. An indirect measurement was also performed to test the delays of the lasing pulse for varying H-atom concentrations. The results show that the lasing pulse exhibits considerable superfluorescence signatures. Analysis based on experimental parameters by using deductive expressions of superfluorescence theory shows good agreement to this conjecture. Our investigations on fundamentals could pave the way to a better understanding of the lasing generation and further applications of lasing-based optical diagnostics.

DOI: 10.1103/PhysRevA.105.013702

I. INTRODUCTION

The lasing effect, i.e., the generation of coherent emission from atoms or molecules by impulsive laser excitation, has been extensively studied in the fields of nonlinear and quantum optics in the 1990s [1–3]. It regained considerable research interest in the last decade because the lasing emission can be generated to propagate backwards to its pump-laser source, which has been deemed to hold great potential applications in standoff diagnostics of combustion and reacting flow as well as the atmospheric environment [4–7]. Two approaches have been found to generate backward lasing, i.e., multi-photon-absorption resonant excitation of atoms or molecules [8–15] and electron-molecule inelastic collision excitation of the neutral nitrogen molecule [16–25], and the first approach is so far the most promising one to generate a backward lasing pulse with μJ-level energy [26]. In this regard, an important milestone was made by Dogariu *et al.*, where lasing from air molecules was demonstrated by using ultrashort laser pulses (100-ps duration) at 226-nm wavelength to consecutively photodissociate oxygen molecules and excite the resultant oxygen atoms via two-photon absorption in ambient air [11]. A single-pass gain coefficient of 62 cm^{-1} was achieved and such high optical gain enabled lasing emission in both forward and backward directions. To date, lasing from atomic species that are created by the dissociation of major air constituents including oxygen [11,13], nitrogen [26], and water molecules [27] has been reported.

The emphasis was put on the methods to generate backward lasing from various atomic species with well-known two-photon-transition schemes. However, much less attention was given to the lasing mechanism. There are mainly two different mechanisms proposed: (1) amplified spontaneous emission (ASE) via stimulated emission process that relates to the population inversion [11,28] and (2) superfluorescence (SF) that requires the presence of both population inversion and the macroscopic dipole (also called atomic coherence) [13,29]. As it is well known, the concept of superradiance (SR) was proposed by Dicke in the first calculation of coherence in the spontaneous emission process in 1954 [30]. It describes cooperative spontaneous emission from a collection of excited atoms or molecules where a macroscopic dipole moment has been initially set up, which manifests as a burst of radiation or a "radiation bomb." Different from SR, SF starts from an initially incoherent superposition of energy levels, which later on spontaneously develops a macroscopic dipole within a characteristic induction time [30]. In this case, normal fluorescence is first emitted by the excitation volume and followed by a SF pulse [31]. In contrast to SF that is a cooperative emission, ASE is a collective emission from an incoherent system. In an ASE process, all the modes of spontaneous emission are amplified by stimulated emission and compete with each other. Gradually the mode with the maximum gain wins out and finally results in a coherent ASE pulse at the end [32]. In practical experiments requiring a pump laser to generate an excitation volume during the propagation, which is the case in the present paper, the phenomena of ASE and SF both appear as cavity-free lasing, and their features are quite similar to each other, namely, a clear pump-laser threshold, spectral line narrowing, low beam divergence, similar polarization inherited from spontaneous emission, and exponential dependence of signal intensity on the pump-laser energy. These common features make it challenging to determine the nature of the observed emission. Conclusive distinction between ASE and SF requires knowledge of excited pop-

*dingpj@lzu.edu.cn
†xues@lzu.edu.cn

Published by the American Physical Society under the terms of the Creative Commons Attribution 4.0 International license. Further distribution of this work must maintain attribution to the author(s) and the published article's title, journal citation, and DOI. Funded by Bibsam.

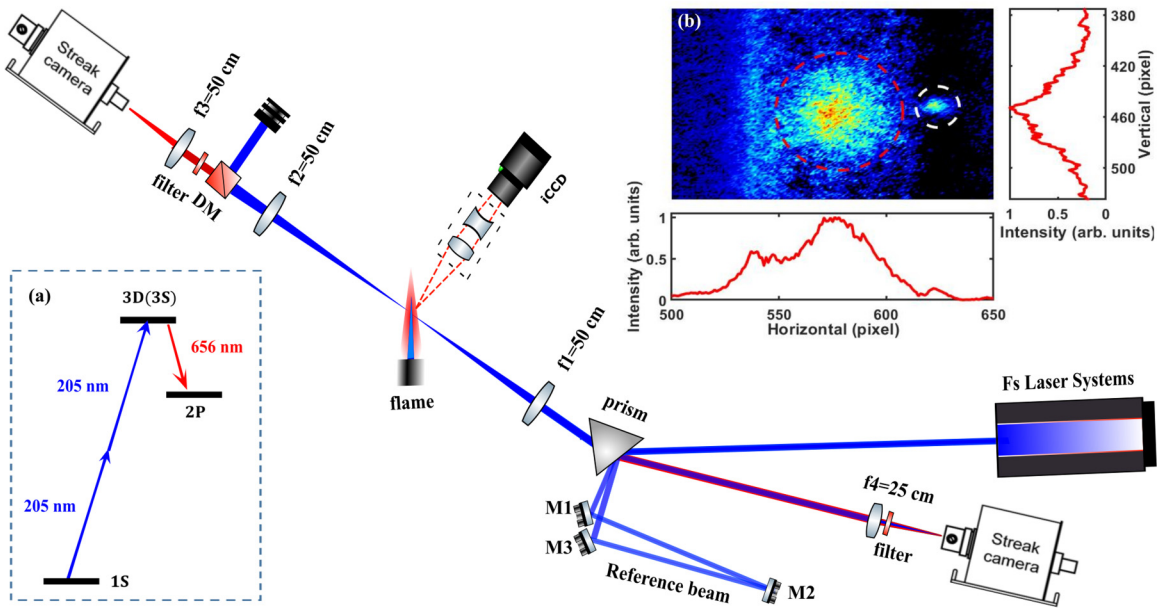

FIG. 1. Schematic illustration of the experimental setup. f, spherical lens; M, ultraviolet enhanced reflective mirror; DM, dichromatic mirror that reflects ultraviolet light and transmits near-infrared light. Insets: (a) Energy diagram of the H atom and the related transitions and (b) records of the backward 656-nm lasing pulse (red circle) and 205-nm reference pulse (white circle) taken by the streak camera in focus mode.

ulation numbers, decoherence time, single-pass gain of the system, etc.

In our previous studies, the generation of bidirectional lasing of H atoms at the Balmer-α line in a premixed CH_4-air flame with femtosecond deep-ultraviolet laser pulses was demonstrated [33–35]. In the excitation scheme, the H atom is excited from 1*S* to 3*D* or 3*S* via resonant absorption of two photons at 205-nm wavelength, followed by down-transition to 2*P* that results in 656-nm radiation [see Fig. 1(a)]. Later on, we found that ASE occurred simultaneously with four-wave mixing (FWM) but ASE dominates in the forward direction, whereas the backward lasing is virtually only ASE [35]. However, it was realized that the evidences presented therein were not able to distinguish if the lasing is fundamentally ASE or SF despite the involvement of FWM since they share a common lasing feature as described above. Recently, Wang *et al.* [36] reported a pump-probe study of forward H-atom lasing in H_2-air flames, in which the gain dynamics were measured, similar to our previous results [see Fig. 4(b) in [35]]. Based on a comparison of the experimental results of gain dynamics for different probe laser energies with the simulations using the theoretical SF model, it was speculated that the H-atom lasing is SF.

In this paper, we performed measurements of the durations of both forward and backward H-atom 656-nm lasing pulses as well as their relative time delays with respect to the pump-laser pulse for varying pump-laser-pulse energies. The results indicate that both the duration and time delay are approximately proportional to the inverse of the pump-laser-pulse energy, suggesting a clear signature of SF. Qualitative analysis based on the SF theory and current experimental parameters show good agreements with the experimental observations. In addition, we conducted qualitative experiments to measure the time delay of the lasing pulse for varying H-atom concentrations in a jet flame. The result exhibits a clear trend that the delay appears shorter with higher concentration, which is in accordance with the typical feature of SF emission.

II. EXPERIMENTAL METHODS

In the experiments, a Ti:sapphire femtosecond laser system (Coherent, Hidra-50) was used to provide approximately 30-mJ, 800-nm laser pulses with a duration of 125 fs, which then pumps an optical parametric amplification system (Light Conversion, TOPAS-PRIME-HE) and a frequency mixing unit (Light Conversion, NirUVis) to generate laser pulses at 205-nm wavelength for exciting H atoms. The laser beam diameter is about 5 mm and the output laser-pulse energy is approximately 60 μJ on average. The schematic of the experimental setup is shown in Fig. 1. The 205-nm laser beam was sent to propagate through a dispersive prism and then focused by a spherical convex lens ($f = 30$ cm) into a premixed welding CH_4-O_2 flame, where H atoms in the ground state are naturally present, generating 656-nm lasing of atomic hydrogen in both forward and backward directions. The size of the excited cylindrical-shaped volume was estimated to be $\approx$100 μm in diameter and $\approx$4 mm in length. The dispersive prism significantly reduces the 205-nm laser-pulse energy due to reflections at its surfaces and internal attenuation, and the maximum pulse energy before the flame was $\approx$20 μJ. The lasing pulses were detected with a spectrometer (Princeton Instruments, Acton SP2500, spectral resolution $\approx$0.018 nm) for measuring the spectra, a streak camera (Optronis, optimal time resolution $\approx$2 ps) for recording the temporal profile, and an intensified charge-coupled device (Princeton Instruments, PIMAX-4) camera for capturing the side fluorescence. Two narrow-band filters (Semrock, $\approx$15-nm bandwidth) with optimal transmission at 656-nm wavelength were placed before

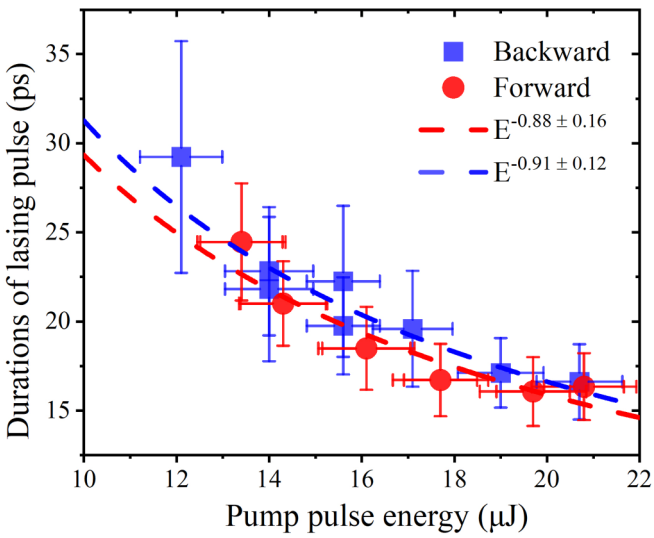

FIG. 2. Durations of forward and backward lasing pulses as a function of the 205-nm pump pulse energies. The dashed lines represent power function fittings.

the detectors. More details of the experimental setup can be found in our previous works [33,35].

The challengeable part of the experiment relates to the method of measuring the time delay of the backward 656-nm lasing pulse with respect to the 205-nm pump-laser pulse. A small portion of the incident 205-nm laser pulse is reflected by the dispersive prism, which is then used as a time reference pulse for the backward lasing pulse. Proper adjustment of the mirror M1, M2, and M3 directs the time reference pulse to propagate alongside with the backward lasing pulse towards the streak camera. M2 was placed on a translational motorized stage to adjust its position. The inset in Fig. 1(b) shows the images of the backward lasing beam and the reference beam taken by the streak camera in its focus mode, in which the streak camera functions as a conventional camera. The beams were deliberately separated to show both of them. In order to determine the position of the M2 mirror, a thin transparent glass is placed at the position of the flame, and the glass is carefully tilted to reflect a tiny portion of the pump-laser pulse back to the streak camera. Then, we simultaneously detected both the reflected pump-laser pulse and the reference pulse with the streak camera, and overlapped these two pulses in time by adjusting the position of the M2 mirror. In this way, the reference pulse functions as the pump-laser pulse in the focus, by which we can obtain the roughly correct time delay of the backward lasing pulse with respect to the pump-laser pulse.

III. RESULTS AND DISCUSSIONS

First, we measured forward and backward 656-nm lasing pulses and studied the dependence of their averaged durations on 205-nm pump pulse energy. The sweeping speed of the streak camera was set to 10 ps/mm and the slit width was fixed to 70 μm, which eventually provides a temporal resolution of approximately 4 ps. The results are shown in Fig. 2. One can notice that the backward lasing pulse is slightly longer than the forward one. Both lasing pulses exhibit a monotonic decrease with the increasing pump pulse energies. The data are fitted with the power function $y = a \times E^b$ through the nonlinear least-squares curve fitting method using the orthogonal distance regression algorithm, where E represents the pump pulse energy and a, b are the fitting coefficients. The fitting suggests a power index of -0.88 ± 0.16 for the forward lasing pulse, and -0.91 ± 0.12 for the backward one.

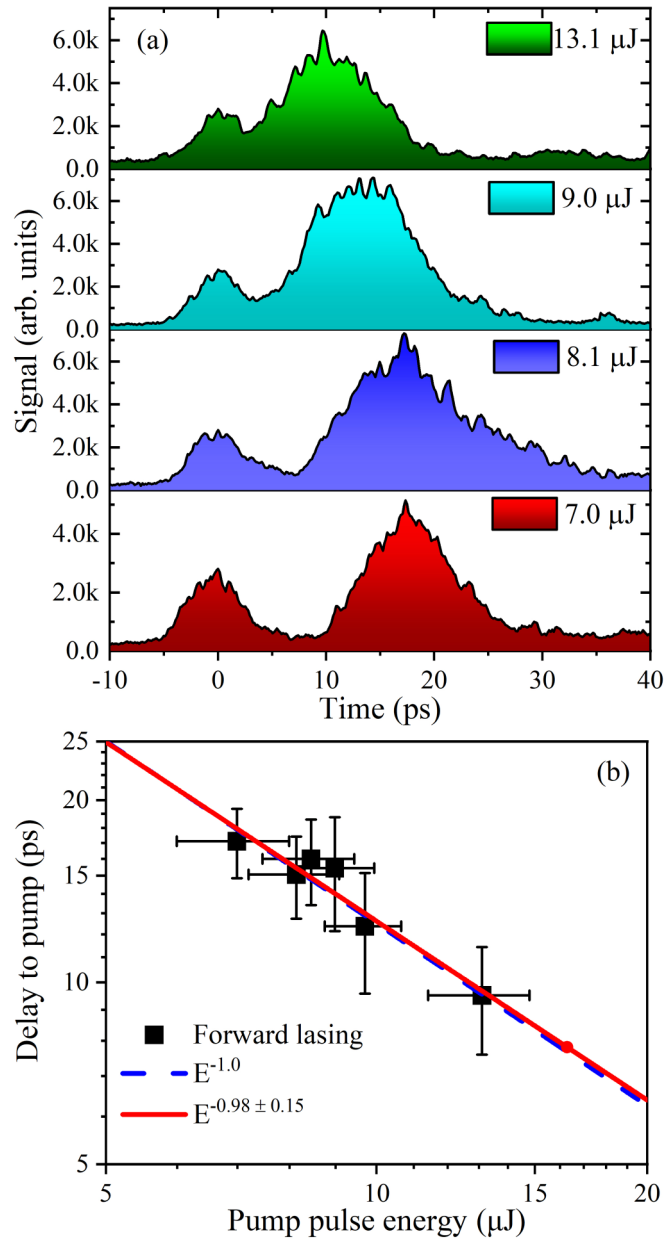

FIG. 3. (a) Temporal profiles of the forward lasing pulses for different pump-laser energies. The pulse at zero time is the 205-nm pump-laser pulse. (b) Delay of the forward lasing pulse as a function of the pump pulse energies. The red solid line represents power function fit whereas the blue dashed line shows exact inverse dependence.

Next, we concentrated on the measurement of the average time delay of the forward lasing pulse with respect to the pump-laser pulse. Figure 3(a) shows the temporal profiles of forward lasing pulses generated with different

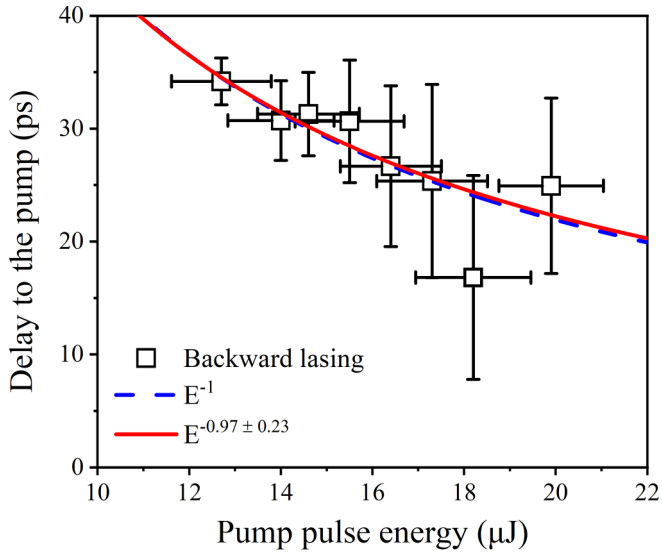

FIG. 4. Delay of the backward lasing pulse with respect to the 205-nm pump pulse as a function of the pump pulse energies.

pump-laser-pulse energies, where the pump-laser pulse was fixed at zero time. Apparently, the forward lasing pulse appears closer to the pump-laser pulse in time as the pump-laser energy increases. The time delay was defined as the temporal separation of the peaks of the pump-laser pulse and the forward lasing pulse, and averaged up to 100 shots. The relative time delay as a function of the pump pulse energy was plotted in Fig. 3(b), from which we can see a monotonic decrease of the delay with increasing pump pulse energy. Power function fitting to the data suggests an index of -0.98 ± 0.15. For the backward lasing, we also managed to measure its time delay with respect to the pump pulse. Compared to the forward lasing, the signal strength of the backward lasing pulse is much weaker. Also, temporal jitter is a complication. These effects lead to a faint signal of the backward lasing pulse appearing in and out of the time window of 192 ps for 10-ps/mm streak speed. Therefore, in order to simultaneously record both the lasing and the reference pulses in the measurements, the streak speed was changed to 25 ps/mm, which substantially increased the signal intensity and also extended the time window to ≈486 ps at the expense of the temporal resolution. Eventually the system gives a temporal resolution of approximately 30 ps, determined by the reference pulse. Figure 4 shows the dependence of delay on the pump pulse energy, which again shows a monotonic decrease with increasing pump pulse energies. Power function fitting to the data suggests an index of -0.97 ± 0.23. The larger error bar in data, compared to forward lasing, is a result of poorer temporal resolution.

Given the limited number of data points, which is a result of the limited range of laser-pulse energies accessible in the current experiments, small deviations of the power indices from a perfect -1 power index are to be expected. Approximately, both the duration (τ) and time delay (τ_d) of the H-atom lasing pulse are proportional to the inverse of the pump pulse energy (E), i.e., $\tau, \tau_d \propto E^{-1}$. With higher laser-pulse energy for pumping, more H atoms are excited to the upper state and contribute to lasing generation. For two-photon excitation, the number of excited atoms (N_e) is proportional to the square of the input laser power, i.e., $N_e \propto E^2$, which was confirmed by the observation that the lasing intensity depends on the square of the pump pulse energy [35]. Therefore, we have $\tau, \tau_d \propto N_e^{-1/2}$, which means that a larger number of excited emitters sets off faster occurrence of the lasing pulse with a shorter duration, a typical signature of SF [12,37].

The occurrence of SF can be characterized with N_e and the single-pass gain αL through the excitation volume of length L [30,31]:

$$\alpha L = \frac{2T_2}{\tau_r}, \tag{1}$$

where T_2 is the collisional dephasing time and τ_r is the cooperative lifetime which gives the typical time scale of SF. For a cylindrical-shaped excitation sample, it was expressed as

$$\tau_r = \frac{AT_1}{\mu N_e \lambda^2}, \tag{2}$$

where $T_1 = 15$ ns [38], $\lambda = 656$ nm, A, and $\mu = 3/8\pi$ are the spontaneous decay time of the excited state, the SF emission wavelength, the cross-section area of the excitation volume, and a geometrical factor, respectively. In the extreme of no collisional dephasing, the SF pulse emits in a duration of the order τ_r with a delay time

$$\tau_d = \tau_r \left[\frac{1}{4}\ln\sqrt{2\pi N_e}\right]^2, \tag{3}$$

with respect to the excitation source [39].

Given the measured single-pass gain coefficient $\alpha = 52\ \mathrm{cm}^{-1}$ in our previous study [35] and the stimulated emission cross section $\sigma_s \sim 2 \times 10^{-12}\ \mathrm{cm}^2$ for the lasing transition [38], the excited number density of the H atom can be estimated to be $n_e = \alpha/\sigma_s = 2.6 \times 10^{13}\ \mathrm{cm}^{-3}$. With the above parameters, we obtain that $N_e = n_e \pi d^2 L/4 \sim 8.164 \times 10^8$, $\tau_r \sim 2.81$ ps, and $\tau_d \sim 21.95$ ps through simple calculations, where the diameter and length of the excitation volume are $d \sim 100\ \mu$m and $L \sim 0.4$ cm, respectively. We can see that the calculated delay is qualitatively in agreement with our measured results (see Fig. 3). It has to be emphasized here that the gain coefficient was measured in a noncollinear geometry so that the real value was definitely underestimated. Assuming a higher gain coefficient, for example, $\alpha = 62\ \mathrm{cm}^{-1}$, that is identical to the gain coefficient of oxygen lasing reported in [11], we obtain $\tau_r \sim 2.35$ ps and $\tau_d \sim 18.68$ ps, which is in better agreement with the experimental result.

Furthermore, with simple calculation we get the measured single-pass gain as $\alpha L \sim 21$ and $\log_{10}\mathrm{N_e} \sim 8.9$. According to the work by Maki *et al.* [40], the SF process can be categorized into different regimes depending on the relative importance of the collisional dephasing, in which the regimes labeled as ASE, damped SF, and SF are separated with the curves $T_2 = (\tau_r \tau_d)^{1/2}$ and τ_d. Thus, the above values of αL and $\log_{10}\mathrm{N_e}$ place the current experiment in the damped SF regime [40], in which both atomic coherence and collisional dephasing play a role. As far as we know, the exact collisional frequency for welding the CH_4-air flame under the atmospheric pressure was not available in literatures. For atomic lasing experiments in air, researchers commonly chose the collisional frequency

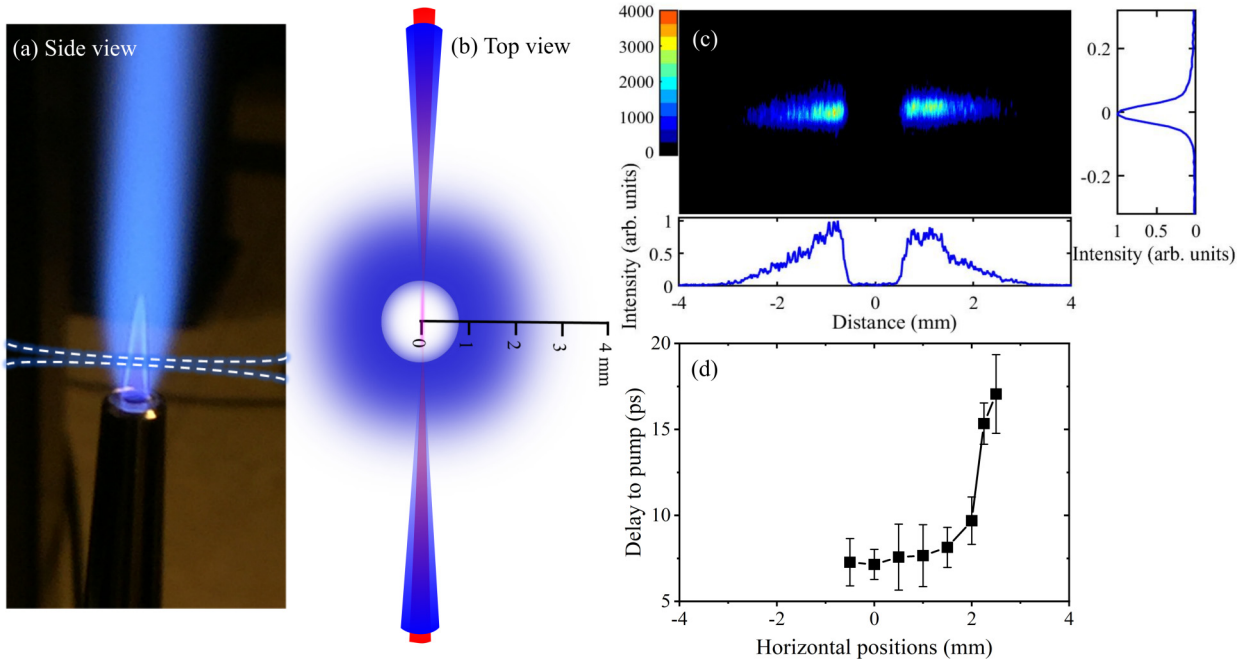

FIG. 5. (a) Side view of the flame structure where the flame fronts can be clearly observed. The dashed line represents laser focusing into the flame. (b) Top view of the experiment configuration. The nebulous cloud illustrates the spatial distribution of H-atom density in the horizontal plane. (c) Single-shot two-dimensional femtosecond two-photon-absorption laser-induced fluorescence (fs-TALIF) imaging of H atoms. Note that similar fs-TALIF imaging has been shown in our previous work [35]. (d) Delay of forward lasing pulses with different horizontal positions in the flame where the 205-nm pump-laser beam was focused.

of $\gamma_{\rm col} \sim 10^{10}$ s^{-1} [13,40]. An earlier work on the measurement of Doppler-free laser-induced fluorescence of atomic oxygen in an atmospheric-pressure CH_4-O_2 flame provided a collisional frequency of $\gamma_{\rm col} \sim 8.0 \times 10^{10}$ s^{-1} [41]. For the CH_4-air flame, a smaller collisional frequency can be expected due to lower flame temperature and we assume a median value as $\gamma_{\rm col} \sim 4.0 \times 10^{10}$ s^{-1}, which results in a dephasing time $T_2 = 1/\gamma_{\rm col} \sim 20$ ps. According to Eq. (1), we get $\alpha L \sim 18$, which is very close to the measured single-pass gain of 21.

The SF regime can be further divided into three regimes labeled as pure SF, weak-oscillatory SF, and strong-oscillatory SF that are separated with the curves $N_e = N_c$ and $N_e = \sqrt{N_c}$ [40], where

$$N_c = \frac{8\pi c T_1 A}{3\lambda^2 L} \tag{4}$$

is the maximum number of atoms that cooperatively emit. With the above formula, we get $N_c \sim 1.72 \times 10^8$, which is a few times lower than N_e. Also, one can calculate $\sqrt{\tau_r \tau_d} \sim$ 7.85 ps, and thus we have $\sqrt{\tau_r \tau_d} < T_2 < \tau_d$. These two results again place the current experiment in the damped SF regime. More importantly, with $N_e > N_c$, the SF theory predicts that the duration and delay time of the SF pulse from the entire excitation volume scale as $N_e^{-1/2}$, which is consistent with the main observations in this paper.

Additional experiments trying to reveal the nature of H-atom lasing were to measure the time delay of the forward lasing pulse for varying H-atom concentrations. Due to the absence of an apparatus to control the H-atom concentration in the excitation volume, we turned to take advantage of the radial distribution of H atoms in the flame as a way of varying its concentration. Figures 5(a) and 5(b) show the side and top views of both the flame structure and the focusing geometry, respectively. From these two abstract graphs, one can clearly catch sight of the flame fronts, where most of the hydrogen atoms are produced through chemical reactions. In order to acquire the precise radial distribution of H-atom concentration in the flame, two-dimensional femtosecond two-photon-absorption laser-induced fluorescence (fs-TALIF) imaging experiments were conducted [42,43] and the result is shown in Fig. 5(c). In the measurements, the height above the burner of the laser focusing spot was kept at ≈7 mm, half the total height of the flame. The fs-TALIF image shows that the H-atom concentration peaks at the radial distance of approximately 1 mm and then quickly decreases down to none at 3 mm. Though a similar image has been reported in our previous work [35], to show it here again is helpful for conveniently acknowledging the spatial distributions of the H-atom atoms.

To study the impact of the H-atom concentration on the lasing pulse, we focused the pump-laser beam at different radial positions to generate forward 656-nm lasing pulses and measured the delays with respect to the pump-laser pulse. Although there are slight variations of both the number of H atoms in the beam path and the gain medium length when the focus position is scanned radially outwards, the overall H-atom concentrations that the pump-laser pulse encountered will decrease with larger radial distance. According to the SF theory, a lower concentration of emitters leads to a longer time delay of the SF pulse with respect to its pump source. Figure 5(d) shows the measured delays of the forward lasing pulses generated at different radial positions, which becomes significantly longer with farther distances from the center of the flame, i.e., with lower H-atom concentration. This result is qualitatively consistent with the SF theory, and thus

provides another, not direct but effective, signature showing that the femtosecond two-photon-excited H-atom 656-nm lasing could be fundamentally SF.

IV. CONCLUSION

To conclude, we have investigated the radiation nature of femtosecond laser-induced H-atom lasing pulses in a flame by measuring the dependences of its duration and delay time on the femtosecond laser-pulse energy. Both the duration and delay time are inversely proportional to the pump-laser energy, showing clear signatures of superfluorescence. This conjecture is further strengthened by a test experiment in which the duration of the lasing pulse decreases with increasing H-atom concentrations. Analysis based on experimental parameters by using deductive expressions of SF theory successfully predicts the delay time and $N_e^{-1/2}$ dependence. Our studies on the radiation nature of femtosecond two-photon-excited atomic lasing contribute to a better understanding of lasing generation, and could be useful for further development of lasing-based optical diagnostics.

ACKNOWLEDGMENTS

This research work was sponsored by the National Science Foundation for Young Scientists of China (Grant No. 12004147), the Knut and Alice Wallenberg Foundation (COCALD Grant No. KAW2019.0084), the European Research Council (TUCLA Grant No. 669466), the Swedish Research Council, and the Swedish Foundation for Strategic Research (Grant No. ITM17-0309).

[1] M. S. Malcuit, D. J. Gauthier, and R. W. Boyd, Suppression of Amplified Spontaneous Emission by The Four-Wave Mixing Process, Phys. Rev. Lett. **55**, 1086 (1985).

[2] J. H. Brownell, X. Lu, and S. R. Hartmann, Yoked Superfluorescence, Phys. Rev. Lett. **75**, 3265 (1995).

[3] W. R. Garrett, Forward Gain Suppression of Optically Pumped Stimulated Emissions Due to Self-Induced Wave-Mixing Interference During a Pump Pulse, Phys. Rev. Lett. **70**, 4059 (1993).

[4] Q. Luo, W. Liu, and S. L. Chin, Lasing action in air induced by ultra-fast laser filamentation, Appl. Phys. B **76**, 337 (2003).

[5] Q. Luo, A. Hosseini, W. Liu, and S. L. Chin, Lasing action in air induced by ultrafast laser filamentation, Opt. Photon. News **15**, 44 (2004).

[6] V. Kocharovsky, S. Cameron, K. Lehmann, R. Lucht, R. Miles, Y. Rostovtsev, W. Warren, G. R. Welch, and M. O. Scully, Gain-swept superradiance applied to the stand-off detection of trace impurities in the atmosphere, Proc. Natl. Acad. Sci. USA **102**, 7806 (2005).

[7] P. R. Hemmer, R. B. Miles, P. Polynkin, T. Siebert, A. V. Sokolov, P. Sprangle, and M. O. Scully, Standoff spectroscopy via remote generation of a backward-propagating laser beam, Proc. Natl. Acad. Sci. USA **108**, 3130 (2011).

[8] M. Aldén, U. Westblom, and J. E. M. Goldsmith, Two-photon-excited stimulated emission from atomic oxygen in flames and cold gases, Opt. Lett. **14**, 305 (1989).

[9] U. Westblom, S. Agrup, M. Aldén, H. M. Hertz, and J. E. M. Goldsmith, Properties of laser-induced stimulated emission for diagnostic purposes, Appl. Phys. B **50**, 487 (1990).

[10] N. Georgiev, K. Nyholm, R. Fritzon, and M. Aldén, Developments of the amplified stimulated emission technique for spatially resolved species detection in flames, Opt. Commun. **108**, 71 (1994).

[11] A. Dogariu, J. B. Michael, M. O. Scully, and R. B. Miles, High-gain backward lasing in air, Science **331**, 442 (2011).

[12] J. V. Thompson, C. W. Ballmann, H. Cai, Z. Yi, Y. V. Rostovtsev, A. V. Sokolov, P. Hemmer, A. M. Zheltikov, G. O. Ariunbold, and M. O. Scully, Pulsed cooperative backward emissions from non-degenerate atomic transitions in sodium, New J. Phys. **16**, 103017 (2014).

[13] A. J. Traverso, R. Sanchez-Gonzalez, L. Yuan, K. Wang, D. V. Voronine, A. M. Zheltikov, Y. Rostovtsev, V. A. Sautenkov, A. V. Sokolov, S. W. North, and M. O. Scully, Coherence brightened laser source for atmospheric remote sensing, Proc. Natl. Acad. Sci. USA **109**, 15185 (2012).

[14] P. Ding, M. Ruchkina, D. D. Cont-Bernard, A. Ehn, D. A. Lacoste, and J. Bood, Detection of atomic oxygen in a plasma-assisted flame via a backward lasing technique, Opt. Lett. **44**, 5477 (2019).

[15] P. Ding, C. Brackmann, M. Ruchkina, M. Zhuzou, L. Wang, L. Yuan, Y. Liu, B. Hu, and J. Bood, Femtosecond laser-induced quantum-beat superfluorescence of atomic oxygen in a flame, Phys. Rev. A **104**, 033517 (2021).

[16] J. Peñano, P. Sprangle, B. Hafizi, D. Gordon, R. Fernsler, and M. Scully, Remote lasing in air by recombination and electron impact excitation of molecular nitrogen, J. Appl. Phys. **111**, 033105 (2012).

[17] D. Kartashov, S. Ališauskas, G. Andriukaitis, A. Pugžlys, M. Shneider, A. Zheltikov, S. L. Chin, and A. Baltuška, Free-space nitrogen gas laser driven by a femtosecond filament, Phys. Rev. A **86**, 033831 (2012).

[18] D. Kartashov, S. Ališauskas, A. Pugžlys, M. N. Shneider, and A. Baltuška, Theory of a filament initiated nitrogen laser, J. Phys. B **48**, 094016 (2015).

[19] S. Mitryukovskiy, Y. Liu, P. Ding, A. Houard, and A. Mysyrowicz, Backward stimulated radiation from filaments in nitrogen gas and air pumped by circularly polarized 800 nm femtosecond laser pulses, Opt. Express **22**, 12750 (2014).

[20] P. Ding, S. Mitryukovskiy, A. Houard, E. Oliva, A. Couairon, A. Mysyrowicz, and Y. Liu, Backward lasing of air plasma pumped by circularly polarized femtosecond pulses for the sake of remote sensing (BLACK), Opt. Express **22**, 29964 (2014).

[21] J. Yao, H. Xie, B. Zeng, W. Chu, G. Li, J. Ni, H. Zhang, C. Jing, C. Zhang, H. Xu, Y. Cheng, and Z. Xu, Gain dynamics of a free-space nitrogen laser pumped by circularly polarized femtosecond laser pulses, Opt. Express **22**, 19005 (2014).

[22] S. Mitryukovskiy, Y. Liu, P. Ding, A. Houard, A. Couairon, and A. Mysyrowicz, Plasma Luminescence From Femtosecond Filaments in Air: Evidence For Impact Excitation with Circularly Polarized Light Pulses, Phys. Rev. Lett. **114**, 063003 (2015).

[23] H. Xie, G. Li, W. Chu, B. Zeng, J. Yao, C. Jing, Z. Li, and Y. Cheng, Backward nitrogen lasing actions induced by femtosecond laser filamentation: Influence of duration of gain, New J. Phys. **17**, 073009 (2015).

[24] P. Ding, E. Oliva, A. Houard, A. Mysyrowicz, and Y. Liu, Lasing dynamics of neutral nitrogen molecules in femtosecond filaments, Phys. Rev. A **94**, 043824 (2016).

[25] P. Ding, J. C. Escudero, A. Houard, A. Sanchis, J. Vera, S. Vicéns, Y. Liu, and E. Oliva, Nonadiabaticity of cavity-free neutral nitrogen lasing, Phys. Rev. A **96**, 033810 (2017).

[26] A. Laurain, M. Scheller, and P. Polynkin, Low-Threshold Bidirectional Air Lasing, Phys. Rev. Lett. **113**, 253901 (2014).

[27] A. Dogariu, T. L. Chng, and R. B. Miles, Remote backward-propagating water lasing in atmospheric air, in *Conference on Lasers and Electro-Optics held in San Jose* (Optical Society of America, Washington, DC, 2016), p. AW4K.5.

[28] P. Polynkin and Y. Cheng, *Air Lasing*, Springer Series in Optical Sciences, Vol. 208 (Springer, New York, 2018).

[29] L. Yuan, B. H. Hokr, A. J. Traverso, D. V. Voronine, Y. Rostovtsev, A. V. Sokolov, and M. O. Scully, Theoretical analysis of the coherence-brightened laser in air, Phys. Rev. A **87**, 023826 (2013).

[30] R. H. Dicke, Coherence in spontaneous radiation processes, Phys. Rev. **93**, 99 (1954).

[31] R. Bonifacio and L. A. Lugiato, Cooperative radiation processes in two-level systems: Superfluorescence, Phys. Rev. A **11**, 1507 (1975).

[32] A. E. Seigman, *Lasers* (University Science Books, Melville, NY, 1986).

[33] P. Ding, M. Ruchkina, Y. Liu, M. Alden, and J. Bood, Femtosecond two-photon-excited backward lasing of atomic hydrogen in a flame, Opt. Lett. **43**, 1183 (2018).

[34] M. Ruchkina, P. Ding, A. Ehn, M. Aldén, and J. Bood, Single-shot, spatially-resolved stand-off detection of atomic hydrogen via backward lasing in flames, Proceedings of the Combustion Institute **37**, 1281 (2019).

[35] P. Ding, M. Ruchkina, Y. Liu, M. Alden, and J. Bood, Gain mechanism of femtosecond two-photon-excited lasing effect in atomic hydrogen, Opt. Lett. **44**, 2374 (2019).

[36] K. Wang, Y. Wang, J. Wang, Z. Yi, W. D. Kulatilaka, A. V. Sokolov, and M. O. Scully, Femtosecond pump-probe studies of atomic hydrogen superfluorescence in flames, Appl. Phys. Lett. **116**, 201102 (2020).

[37] G. O. Ariunbold, M. M. Kash, V. A. Sautenkov, H. Li, Y. V. Rostovtsev, G. R. Welch, and M. O. Scully, Observation of picosecond superfluorescent pulses in rubidium atomic vapor pumped by 100-fs laser pulses, Phys. Rev. A **82**, 043421 (2010).

[38] R. Auyeung, D. Cooper, S. Kim, and B. Feldman, Stimulated emission in atomic hydrogen at 656 nm, Opt. Commun. **79**, 207 (1990).

[39] D. Polder, M. F. H. Schuurmans, and Q. H. F. Vrehen, Superfluorescence: Quantum-mechanical derivation of Maxwell-Bloch description with fluctuating field source, Phys. Rev. A **19**, 1192 (1979).

[40] J. J. Maki, M. S. Malcuit, M. G. Raymer, R. W. Boyd, and P. D. Drummond, Influence of collisional dephasing processes on superfluorescence, Phys. Rev. A **40**, 5135 (1989).

[41] M. J. Dyer and D. R. Crosley, Doppler-free laser-induced fluorescence of oxygen atoms in an atmospheric-pressure flame, Opt. Lett. **14**, 12 (1989).

[42] D. D. Cont-Bernard, M. Ruchkina, P. Ding, J. Bood, A. Ehn, and D. A. Lacoste, Femtosecond two-photon laser-induced fluorescence imaging of atomic hydrogen in a laminar methane-air flame assisted by nanosecond repetitively pulsed discharges, Plasma Sources Sci. Technol. **29**, 065011 (2020).

[43] P. Ding, M. Ruchkina, D. D. Cont-Bernard, A. Ehn, D. A. Lacoste, and J. Bood, Temporal dynamics of femtosecond-TALIF of atomic hydrogen and oxygen in a nanosecond repetitively pulsed discharge-assisted methane–air flame, J. Phys. D **54**, 275201 (2021).

Correction: The copyright license statement was presented incorrectly and has been fixed.